The Cole relaxation frequency as a parameter to identify cancer in breast tissue

W. D. Gregory[a)]
College of Engineering and Applied Sciences and College of Health Sciences, University of Wisconsin, Milwaukee, Wisconsin 53211 and NovaScan, LLC, Milwaukee, Wisconsin 53233

J. J. Marx
Aurora Health Care, Milwaukee, Wisconsin 53233

C. W. Gregory
NovaScan, LLC, Milwaukee, Wisconsin 53233

W. M. Mikkelson and J. A. Tjoe
Aurora Health Care, Milwaukee, Wisconsin 53233

J. Shell
NovaScan, LLC, Milwaukee, Wisconsin 53233

(Received 11 August 2011; revised 2 May 2012; accepted for publication 16 May 2012; published 18 June 2012)

Purpose: To correlate the Cole relaxation frequencies obtained from measurements of the electrical properties of breast tissue to the presence or absence of cancer.
Methods: Four-lead impedance measurements were obtained on *ex vivo* specimens extracted during surgery from 187 volunteer patients. Data were acquired with a commercial Solartron impedance bridge employing 4-lead Ag–AgCl or blackened platinum (BPt) electrodes at frequencies logarithmically spaced from 1 Hz to 3.2×10^7 Hz utilizing 6–10 frequencies per decade. The Cole frequencies obtained from these measurements were correlated with the tissue health status (cancer or noncancer) obtained from histological analysis of the specimens.
Results: Analysis of the impedance measurements showed that the Cole relaxation frequencies correlated to the presence or absence of cancer in the examined tissue with a sensitivity up to 100% (95% CI, 99%–100%) and a specificity up to 85% (95% CI, 79%–91%) based on the ROC curve of the data with the Cole frequency as the classifier.
Conclusions: The results show that the Cole frequency alone is a viable classifier for malignant breast anomalies. Results of the current work are consistent with recent bioimpedance measurements on single cell and cell suspension breast cell lines. [http://dx.doi.org/10.1118/1.4725172]

Key words: bioimpedance, Cole–Cole, relaxation frequency, breast cancer, biomedical

I. INTRODUCTION

Characterization of the bio-electric properties of human tissue was made possible by the work of Cole *et al.* who produced an equivalent circuit to model biological impedance behavior.[1,2] This equivalent circuit (embodied in the Cole function, Eq. (1) below) typically models the spectral data with four parameters including the relaxation frequency,

$$\boldsymbol{Z} = \frac{R_1 - R_3}{1 + \left(j\frac{f}{f_c}\right)^{\alpha}} + R_3, \tag{1}$$

where bold quantities are complex and nonbold quantities are real numbers; $\boldsymbol{Z}$ is the complex sample impedance where Zp is the real or resistive part of $\boldsymbol{Z}$, and Zpp is the imaginary or reactive part; real parameters R_1 and R_3 represent the low and high frequency limits of $\boldsymbol{Z}$, respectively; f is the measurement frequency; and f_c is the Cole relaxation frequency, both in Hz; $j = \sqrt{-1}$; and α is a dimensionless number that is inversely related to the broadening in the frequency domain of Zp, and the spread of the peak seen in $-Zpp$.

Gabriel *et al.*[3,4] have collected a large body of data on the electrical properties of human tissue from the literature and parameterized the data by fitting to multiple Cole functions. The Gabriels' work has demonstrated that Cole parameterization results describe different human tissue types (muscle, fat, skin, etc.) and different regions of frequency response (dispersion regions) as defined by Schwan[5] labeled: α (From 10^1 Hz to $\sim 10^3$ Hz), β (from 10^3 to $<10^7$ Hz), δ ($<10^{10}$ Hz), and γ ($>10^{10}$ Hz). Each of the dispersion regions is attributed to different frequency dependent phenomena in the tissue.[6] Schwan identified 12 biomaterial elements that can be probed by bioimpedance measurements in the various dispersion regions (see Fig. 1).[7] Of these, 11 of the 12 biomaterial phenomena can be observed in the β region, 6 in the γ region, and 5 in the α and δ regions. Most importantly, only the β region allows measurement of properties of the vesicles and the cell materials with membranes. Because our interest was to probe the cell and cell membrane response to an applied electric field, we concentrated on the β region from about 10^3 Hz to 10^7 Hz.

CONTRIBUTING BIOMATERIAL ELEMENT		DISPERSION α	β	γ	δ
Water and Electrolytes				•	
Biological Macromolecules	Amino Acids		•	•	•
	Proteins		•	•	•
	Nucleic Acids	•	•	•	•
Vesicles	Surface Charged	•	•		
	Non-Surface Charged		•		
Cellular Membrane	Fluids free of protein		•		
	Tubular system	•	•		
	Surface Charged	•	•		
	Membrane relaxation	•	•		
	Organelles		•	•	•
	Proteins		•	•	•

FIG. 1. Tissue bioimpedance frequency response dispersion regions as shown in Portero (Ref. 7), derived from Schwan (Ref. 5).

A practical application of the parameterization of electrical properties of tissues is the detection and diagnosis of cancer. Over the past two decades numerous studies of breast cancer tissue in the β dispersion region have been conducted, but agreement has not been reached on the most reliable parameters for distinguishing cancerous from noncancerous breast tissues using electrical properties. Jossinett and Schmitt[8] measured the admittance of freshly excised breast tissue and concluded that, although they found that differences in admittance parameters distinguish cancerous from other types of tissues, no single parameter alone was sufficient for discrimination of any one tissue type. Chauveau *et al.*[9] measured breast tissues and reported that the conductivity, the characteristic frequency, and the shape of the Bode plots were the best predictors for distinguishing cancerous from noncancerous tissue. Wang *et al.*[10] developed a classification method using five parameters, which are projection slopes; the center coordinates of the Cole-Cole curve; the area ratio of a difference curve defined in the paper; the fitting slope of the difference curve; and the span of the difference curve. Wang *et al.*[11] performed an *ex vivo* impedance spectroscopy experiment and showed that the resistivity of various breast tissues exhibit the following pattern: adipose tissue > cancerous tissue > mammary gland and benign tumor tissue. Estrela *et al.*[12] used statistical analysis to derive a set of rules based on features extracted from the graphical representation of electrical impedance spectra. These rules were used hierarchically to discriminate several classes of breast tissue.

Perhaps the most comprehensive studies of the electrical bioimpedance of human breast tissue have been conducted by two groups. The Paulson[13,14] group at Dartmouth has reported studies both in the laboratory and in a clinical setting, comparing *ex vivo* and *in vivo* data.[15] Conductivity and permittivity were measured in *ex vivo* samples over the frequency range from 100 Hz to 8.5 GHz. The Hagness group at the University of Wisconsin has reported results in the microwave region for tissue from patients with breast disease[16] and in a separate paper[17] from patients undergoing breast reduction.

The current paper differs from this previous work in that we distinguish cancerous from noncancerous breast tissue by the use of a single parameter, the Cole relaxation frequency. Most of the previous work used multiple parameters to distinguish healthy and cancerous tissue. A related difference is that many of the previous reports utilized admittance or impedance values as part of the classification scheme. That choice can be problematic, since a complicated heterogeneity of tissue types can produce an average value that is in the range of yet another tissue type that is not actually present. This can cause either a false positive (if the average data are in the range of the sought after classification), or a false negative (if one of the admixture of tissue types was, in fact, the sought after classification). We found the separation of tissue types was better accomplished in the frequency domain. This choice required a detailed investigation of the bioimpedance spectra of numerous specimens and the development of a method of analysis to untangle overlapping relaxation impedance spectra found in inhomogeneous samples. These analyses are reported herein.

II. METHODS

II.A. Clinical protocol

The *ex vivo* measurements reported here are part of a continuing long term Institutional Review Board (IRB) approved study (beginning in 2004 and renewed annually) at the Aurora Health Care hospitals in Milwaukee, WI, with the goal of developing a database of breast tissue electrical properties obtained from excised breast tissue.

In accordance with the approved IRB protocol for this study, we enrolled patients based on the presumptive diagnosis of a disease process ongoing in the breast. Measurements of a patient's samples were subsequently included in this analysis if the histological diagnosis of the disease from examination of microscope slides of the tissue samples included combinations of invasive ductal and/or lobular carcinoma with or without ductal or lobular carcinoma *in situ* (DCIS or LCIS), and DCIS or LCIS alone. Samples of such tissue are referred to as cancer (CA) in this paper. Patients with a pathologic description of benign breast disease (BBD) including a confirmed diagnosis of Fibroadenoma, noninfiltrating papilloma, and nonspecific tissue reaction without malignant or atypical cells, were excluded from this analysis. Cases of atypical ductal or lobular hyperplasia also were not included in this analysis. Fibroglandular tissue in a matrix of adipocytes was considered "normal ductal" tissue (DU).

Immediately following a surgical lumpectomy or mastectomy, the excised tissue was taken to the histology laboratory for gross margin analysis, processing, and sectioning of the tissue. The histology laboratory provided fresh tissue samples as follows: (1) a portion of the cancerous (CA) lesion(s) and (2) glandular (ductal and lobular) rich tissue (DU) 5 cm from a region outside the closest tumor margin. (These abbreviation designations and definitions are used throughout this paper.) To minimize concerns that ischemic changes of the tissue would alter our results if the tissue was not examined immediately after excision,[18,19] a research team member received the freshly excised tissue in the surgery suite and carried the tissue to the histology laboratory. The elapsed time from

excision to beginning impedance measurements was thus kept to a minimum, usually less than 10 min.

CA and DU samples provided by the pathology laboratory personnel were large enough to cover the 1 cm square surface area of the electrodes and ranged in size from 1–2 cm^2 to 3–4 mm deep. On occasion, the size of the tumor for a given patient was so small that the pathologist could not provide us with tissue from the tumor without compromising the ability to make enough microscope slides to achieve a suitable diagnosis. On other occasions tissue from regions greater than 5 cm from the tumor margin could not always be obtained because the partial mastectomy was not large enough (this occurred for about 30% of the patients). For these reasons, the net numbers of CA and DU samples were not equal. Also, at times we would measure the bioimpedance of several CA samples for a given patient if there was uncertainty regarding the histological character of a tissue. These different regions were marked separately, counted as separate samples, but still attributed to a given patient.

After completion of the impedance measurements, each sample was returned to the laboratory where a pathologist would examine microscopic slides of each specimen and issue a pathology report. Pathology results were then compared to the impedance measurement results.

II.B. Apparatus and measurement technique

The measurement fixture consisted of 4-lead electrodes, 4 mm long, 0.5 mm in diameter parallel circular cross-section rods aligned in a straight-line array separated by 2 mm (center-to-center) between adjacent electrodes. Two different electrode configuration geometries and two different electrode surface treatments were employed.

Geometries: (a) with electrodes perpendicular to the tissue to be measured so that they could be inserted into the tissue specimen; or (b) with the same electrodes bent and made parallel to the tissue surface so that measurements could be made by smoothly moving the electrodes across the specimen. Data were taken with both types of electrodes and the results were comparable.

Surface treatments: (a) silver-silver chloride (Ag–AgCl) or (b) blackened platinum (BPt). Both were equally effective in reducing electrode polarization (EP) effects.[20]

A previous paper reported that the effect of breast cancer on the measured electrical properties of tissue can be very pronounced over small distances[21] in the tissue near a tumor. For the impedance data collected with injection type electrodes we were able to obtain a one-to-one correspondence between the region of interest (ROI) examined by the pathologist and the ROI measured electrically. This is because injection electrodes produce indentations in the tissue that can be seen under a microscope, confirming the ROI agreement between our data measuring volume and the pathology analysis. For data acquired using the sliding type electrodes, we used the standard coloring agents for marking histology specimens to indicate the electrical impedance ROI.

To determine whether the tissues were exhibiting changes in the Cole relaxation frequency during the subsequent impedance measurements, we took three sample measurements over time, recording the times of each measurement as part of the computer file data. These observations confirmed that the Cole relaxation frequency did not change measurably during our measurements (less than 6% of the Cole frequency for measurements that took 15 min). We also found that some short time changes in the impedance plots occurred when the electrodes were placed in a sample. Using calibrated conductivity electrolyte solutions held at various fixed temperatures, we traced these changes back to the electrodes taking some time to equilibrate to media that differed in temperature and/or conductivity. Based on the results of these design experiments, we accepted as our final measurement one in which equilibrium had been reached and there was no observable change in the impedance plot from the previous measurement.

Having developed an acceptable experimental sample-handling protocol, we moved to analyzing the electrical response of our apparatus. To do this we measured the electrical properties of tissue samples at frequencies from 1 Hz to 3.2×10^7 Hz using a Solartron 1260A impedance-phase/gain analyzer.[22] A considerable effort was devoted to correct the Solartron frequency response for observed high frequency anomalies due to front-end loading (leakage currents) and roll-off of the input voltage amplifiers. We also conducted experiments with calibrated concentration electrolyte solutions to confirm our designation of some impedance features as artifacts and some as true response of the tissue cells. Finally, we developed a number of software tools to compare our data to the Cole function, Eq. (1). Among these, we used a nonlinear minimization routine developed by Powell[23] to obtain the best fit of the Cole function parameters to the data. More of the technical details regarding the hardware and software used in this work will be described in a future paper.

III. RESULTS

To date we have analyzed 232 CA and 141 DU specimens from the 187 volunteer patients. Figure 2 shows the results from a fit of the Cole function to the impedance measurements of excised breast tissues for two cases: Fig. 2(a) is a plot of Zp and Zpp of a DU (ductal) tissue sample, Fig. 2(b) is a similar plot for a CA (cancerous) region. In these figures, we also show f_c, α, and the Pearson correlation values of the fit of the data for each component to Eq. (1). For these two samples, the Cole relaxation frequency is noticeably different.

An effective parameter for determining the health status of breast tissue requires an accurate means of measuring this parameter. Tissue impedance data are strongly affected by the Cole frequency as a fitting parameter over the entire frequency domain, with one characteristic point (the peak in $-Zpp$) occurring exactly at the Cole frequency. As we examined a large amount of data, we found that our data comprised a rich set of phenomena, ranging from: (a) data with a single time constant or Cole frequency (F_{cole}) comparable to the almost ideal Cole plots of Fig. 2; (b) cases with separable multiple Cole peaks of Fig. 3; and (c) more complex data with a variety of large and

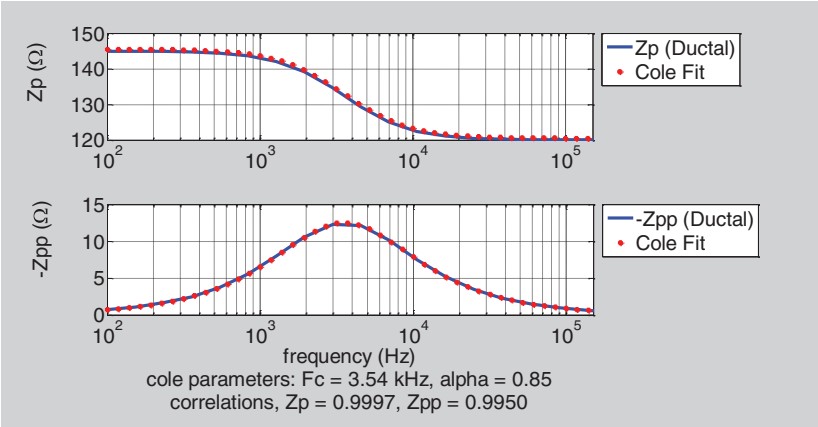

(a)

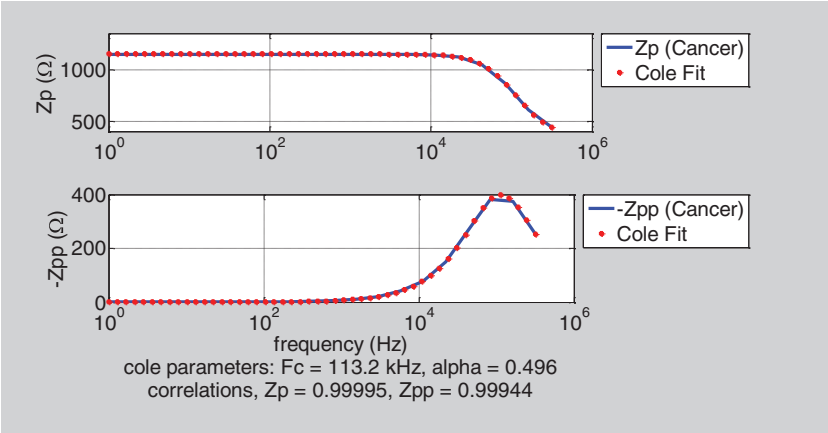

(b)

FIG. 2. Comparison of the impedance components vs frequency from 10^2 to 10^6 Hz for two samples: (a) a DU sample (tissue with high ductal material content excised about 5 cm from the tumor margin), and (b) a CA sample (tissue from the interior of a cancerous tumor). The Cole parameters α, f_c, and the Pearson correlation values for the fit of each component are provided.

small magnitude excursions displaying overlapping Cole-like contributions. We developed the following procedures to determine the Cole frequencies for each of these types of data:

a. *Single peak data* (41% *of the data*): For data with well separated peaks in $-Zpp$, 90.9% have a Pearson correlation value to the Cole function for Zp of 0.99 or better, and 98.6% of 0.9 or better, while for $-Zpp$, 81.0% have a correlation of 0.99 or better and 97.3% have a correlation of 0.9 or better. For these cases, the Powell minimization procedure can be trusted to return a mathematical "best fit" that is physically tenable producing positive values for the Cole fit parameters (i.e., $f_c > 0$; $0 < \alpha < 1$; R_1 and $R_3 > 0$).

b. *Multiple distinct peak data* (33% *of the data*): When a small number of peaks in $-Zpp$ are present and are close together, we found that fitting two or three Cole functions to the data will unfold the overlap of the $-Zpp$ maxima or minima and generate a precise fit of the experimental and theoretical curves using the Powell procedure that are also physically reasonable, a similar finding to that of Gabriel *et al.*[4] Figure 3 is an example of a case where there are two contributing portions to the measured $\boldsymbol{Z}$ of a tissue specimen that are fit using two Cole functions. Figure 3(a) is a plot of the Zp component of the impedance for the experimental data, each of the two contributing portions, and the theoretical sum of the contributing portions. Figure 3(b) is a similar plot for the Zpp component.

c. *Complex peak frequency distributions* (26% *of the data*): Finally, yet another class of data was identified that showed multiple overlapping peaks in $-Zpp$. In those cases, we made use of a unique feature of the Zp component of the data: the region on either side of the frequency point where $-Zpp$ peaks (i.e., where $\frac{f}{f_c} = 1$) is linear vs $\log_{10}(\frac{f}{f_c})$, to a very good approximation, even when the $-Zpp$ peak is difficult to identify and seemingly convoluted. By selecting the middle of the range of frequencies where Zp is linear in $\log_{10}(\frac{f}{f_c})$ to identify each f_c value, we obtained a set of Cole frequencies for a given specimen. We used an interactive computer program to fit the data to both components of $\boldsymbol{Z}$ to multiple Cole functions with each of those f_c values, verifying these choices as Cole function contributions to the overall impedance of the specimen.

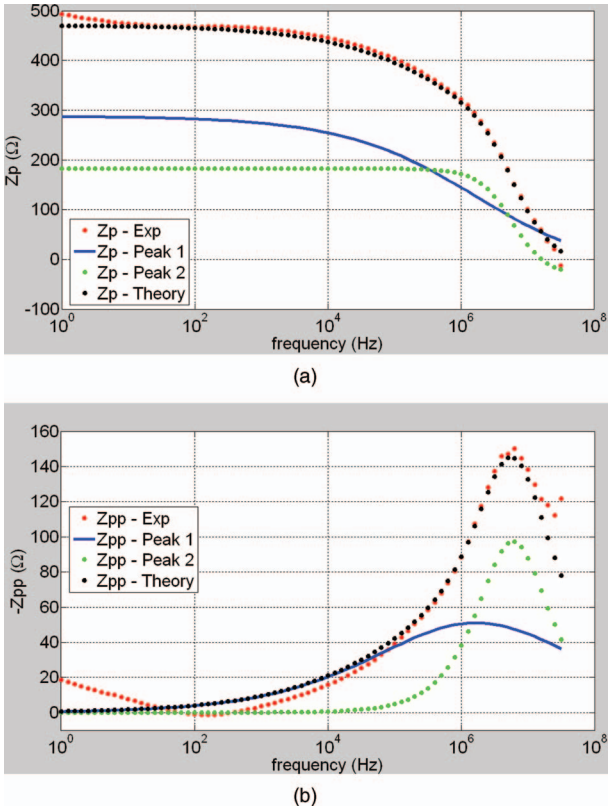

FIG. 3. An example of a case where there are two peaks in $-Zpp$ that are fit using two Cole functions. (a) A plot of the Zp component of the impedance for 4-lead experimental data, each of the two contributing peak elements, and the theoretical sum of the contributing peaks. (b) A similar plot for the $-Zpp$ component.

We have used the methods mentioned above to analyze our data, first with data that had clearly separated Cole peaks, or overlapping peaks separable with the methods (a) and (b) above. That analysis was undertaken by three researchers and repeated about 5 times, in whole or part. Recently, we perfected the broader semiautomatic technique (c) and two researchers expanded the analysis to subsets of the data amenable to all three methods. In cases where we observed a broad smearing of the Cole plots vs frequency, we assigned a range of frequencies to F_{cole} that encompassed this spread. A specimen was classified as CA if a portion of this range of frequencies overlapped with the spread of CA frequencies found for other cases using methods (a) and (b).

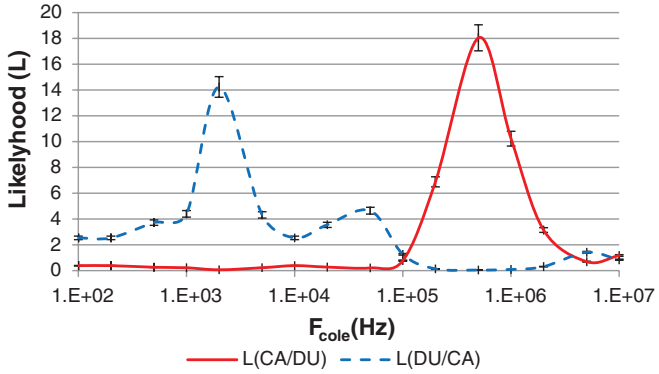

FIG. 5. Likelihood distributions of CA and DU designations based on the distribution of Cole frequency values.

To test the hypothesis that the health status of breast tissue is correlated with the Cole frequency obtained from impedance measurement of the tissue we have created histograms of these Cole frequencies. It is well known that care in the use of histogram analysis requires choosing an optimum bin width. The Sturges[24] and Scott[25,26] rules for bin widths are applicable to the smaller datasets discussed here. They predict an optimum bin width of the order of one bin per decade of frequency, which we found produced reasonable distribution shapes without the erratic behavior caused by overly small choices of bin width. The Freedman-Diaconis[27] rule applies to larger datasets and was not useful for this work.

Figure 4 is a histogram of the number of samples per Cole frequency (F_{cole}) derived from analysis of the impedance data for 232 CA samples and 141 DU samples. The data for each tissue type were normalized to a standard total of 100 normalized (Norm) values. We computed the mean values of each data bin and the standard error of these mean values. We used

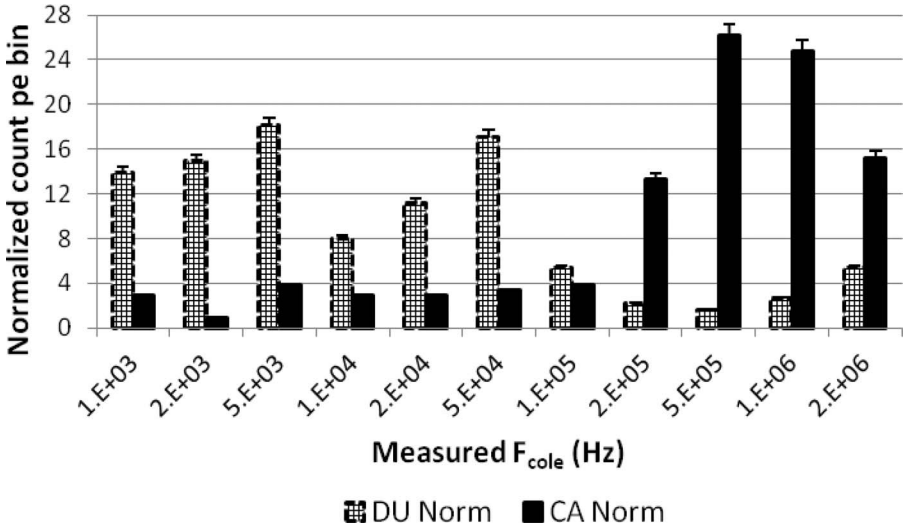

FIG. 4. Histogram plots of the distribution of the Cole relaxation frequency values, F_{cole}, for CA and DU samples.

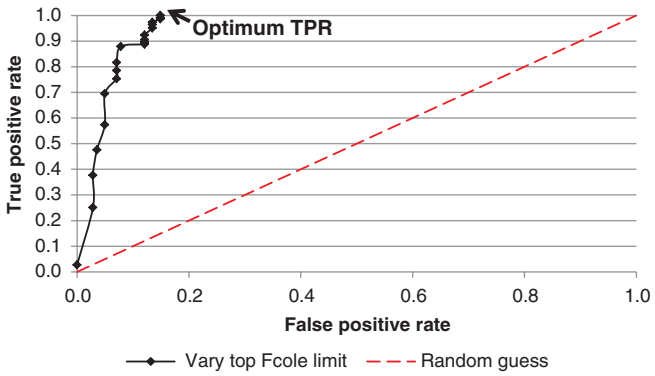

FIG. 6. ROC curve based on the Cole frequency as the classifier over the frequency range from 1×10^{05} to 2×10^{06} Hz. The ROC curve was generated by reducing the upper limit (2×10^{06} Hz) in steps till the lower limit (1×10^{05} Hz) was reached. The optimum sensitivity and specificity are indicated on the plot, with a more complete listing of the optimum statistics shown in Table I.

these data to estimate the repeatability of each data bin as 4% as described by Cumming *et al.*[28] The error bars in the plot are set at that value.

The data in Fig. 4 are a measure of the relative distribution functions of CA and DU Cole frequency values at a number of histogram bin frequencies. Figure 5 is a likelihood plot obtained from taking the ratios of the distribution functions at each histogram center frequency to illustrate the relative likelihood that one will find CA or DU in a given frequency regime. The error bars in the likelihood plots are 5.6%, computed from the combined errors of the division of the distribution function values for each frequency bin. From these plots we developed a criterion for designating cancer as more likely when the Cole frequencies (or a portion of the spread in the Cole frequency values) are in the range of 10^5 Hz–2×10^6 Hz. A noncancer designation is more likely if the Cole frequencies are in the range of 10^3 Hz–10^5 Hz. Figure 6 is a ROC plot of these data wherein the top Cole frequency of 2×10^6 Hz was reduced in steps and the true positive rate (TPR) and false positive rate (FPR) were recomputed as a classifier of our CA (cancer) vs our DU (ductal) samples. As indicated on the plot, the optimum TPR value is 1.0 or 100%. Further statistical data for this optimum point are listed in Table I.

TABLE I. Diagnostic two level test for cancer and ductal.

	Cancer	Ductal	95% CI
Positive	232	21	
Negative	0	120	
Sensitivity	100%		99%–100%
Specificity	85		79%–91%
Pretest probability	62		57%–67%
Positive predictive value	92		88%–95%
Negative predictive value	99		98%–100%
Likelihood ratio (+)	6.69		4.51–9.92
Likelihood ratio (−)	0.01		0.00–0.04

IV. DISCUSSION AND CONCLUSIONS

In this paper we have examined the use of the Cole relaxation frequency as a classifier to find cancerous breast tissue. We found that the Cole relaxation frequency is an excellent indicator of the presence of breast cancer. The salient result of these measurements is the conclusion that cancerous tissue was shown to have a Cole relaxation frequency between about 10^5 Hz and 2×10^6 Hz.

In comparison to previous work cited earlier,[1–16] we note that the work reported here differs primarily in the concentration on a single parameter classification scheme (the Cole relaxation frequency) and the subsequent need to separate Cole frequencies from samples of mixed tissue types, or nonperfect tissues. Jossinett and Schmitt,[8] Wang *et al.*,[11] and Chauveau *et al.*[9] all describe various types of tissue components found in the breast. In particular, Chauveau *et al.* observed many types of data that we have also seen in the samples where it is more difficult to separate out multiple Cole relaxation frequencies. They have identified some of these as specimens that exhibit substantial fibrocystic changes, an identification that agrees with our observations. In these more challenging specimens, the Cole function [Eq. (1)] is often inadequate to describe the large spread of relaxation frequencies with a single Cole function and associated parameters. We are conducting a theoretical investigation of alternate methodologies to solve this problem.

We have not found a study of intact *ex vivo* or *in vivo* breast tissue that delineates the same range of Cole frequencies (1×10^5–2×10^6 Hz) as we have associated with the presence of breast cancer. However, we do cite here two recent studies of four breast cell lines that support this conclusion. These studies used cells suspended in phosphate buffered electrolyte solution (PBS). The cell lines used in those studies are: benign human breast tissue cell line MCF-10A, early-stage breast cancer cell line MCF-7, invasive human breast cancer cell line MDA-MB-231, and metastasized human breast cancer cell line MDA-MB-435. Han *et al.*[29] measured the magnitude and phase of the response of single cells from each cell line. These were single cells suspended in PBS trapped between electrodes in a microfluidic device. The measurements were made over a frequency range from 10^2 to 3×10^6 Hz. The magnitude of the impedance exhibited a strong power law dependence on frequency for disease free cells (MCF-10A) ($[\text{frequency}]^{(-2.5)}$). For each of the other cell lines the exponent in the power law was smaller than 2.5, decreasing from MCF-7 to MDA-MB-231, and finally to MDA-MB-435 where the impedance magnitude was essentially a constant ($[\text{frequency}]^{(-0.0)}$). We interpret this as a reduction in polarizability of the cells as they transform to cancer.

If the polarizability of breast tissue reduces in cancer specimens, as Han *et al.* apparently found, then one would also expect the effective time constant of the tissue to change, based on this simple model: with the time constant of the tissue defined as a resistance, R, times a capacitance, C, associated with the relaxation time constant in the cell (τ), C will be smaller if the polarizability is smaller, so the time constant ($\tau = RC$) will be smaller and thus the relaxation frequency

higher. This is indicative of a change from a polarizable to a nonpolarizable cell with respect to the suspension medium.

The measurements of Qiao *et al.*[30] support this hypothesis. They measured the overall average impedance values for the same cell lines in the same suspension fluid as Han *et al.* and found that the Cole relaxation frequency changed from 3.1×10^5 to 1.01×10^6 Hz from the disease free to the metastatic cancer cell lines, respectively, which fits within the frequency range we have associated with cancerous tissue in this paper. When we further postulate that the cell lines will likely have more uniformity than the full tissue *ex vivo* specimens, this would explain why the spread of "cancer" Cole frequencies is smaller for the cell lines.

The observation that we see cancerlike values for peaks in $-Zpp$ where there are no identifiable cell morphology changes under the microscope might result from the inability to observe precancerous cell changes in typical histologic observations for cell components smaller than the 200 nm limit of optical imaging. Subramanian *et al.*[31] have recently shown that one can observe disorder in the nanoarchitecture for cell components much smaller than the optical limit using partial wave analysis. In particular, they have shown that this disorder is present in both transformed and nontransformed cells in colon cancer patients but not in noncancer patients. Another possibility that may account for the Cole frequency determinations similar to cancer cells might be the presence of low levels of transformed cells dispersed throughout the normal tissue. Since most of these results occurred in the normal tissue areas of patients with invasive disease cancer, occult cells may be present deeper in the tissue not visible to a surface analysis as is performed in most pathology laboratories. Although these authors think this as an unlikely scenario, the possibility cannot be discarded. Perhaps occult tumor cells contribute just sufficient signal to the Cole frequency determination to indicate the presence of these cells despite their apparent absence in the visible examination. In support of this hypothesis, at least half of the samples indicating a "false positive" signal had defined areas outside the margin of the invasive tumor, and one additional sample had evidence of lymphovascular invasion associated with the tumor area, although not apparent in the ductal sample measured.

ACKNOWLEDGMENTS

This paper is based upon work supported in part by the National Science Foundation under Award Nos. 0944454 and 1058413. Any opinions, findings, and conclusions or recommendations expressed in this paper are those of the authors and do not necessarily reflect the views of the National Science Foundation. In addition, we received support from the University of Wisconsin-Milwaukee; Aurora Health Care Inc.; NovaScan, LLC; the Wisconsin Institute for Biomedical and Healthcare Technologies; and CAMCARE, the research and education foundation of the Charleston Area Medical Center, Charleston, WV. The WiSys subsidiary of the Wisconsin Alumni Research Foundation and the University of Wisconsin System supported a portion of this work. The authors are grateful to their colleagues at the University of Wisconsin, Milwaukee (S. Sheerin, M. Stoneman, and V. Raicu), Marquette University (C. Steinmetz), Aurora Health Care (C. Davis and C. Halliday), and NovaScan (P. Voith, and A. Nichols) for their assistance. The authors are particularly indebted to D. McRae and T. Bernstein for a careful review of the manuscript for this paper.

Certain intellectual property related to the results reported here have been assigned by the University of Wisconsin-Milwaukee to WiSys, a subsidiary of WARF, the patent licensing arm of the University of Wisconsin System. WiSys has, in turn, granted exclusive license for this intellectual property to NovaScan, LLC. W. D. Gregory, C. W. Gregory, and Aurora Health Care have financial interests in NovaScan LLC, but the Aurora Health Care personnel, J. J. Marx, W. M. Mikkelson, and J. A. Tjoe, have no derived interest.

[a]Author to whom correspondence should be addressed. Electronic mail: wdguwm@aol.com

[1]K. Cole and R. Cole, "Dispersion and absorption in dielectrics," J. Chem. Phys. **9**, 341–351 (1941).
[2]K. Cole and H. Curtis, "Electrical physiology: Electrical resistance and impedance of cells and tissues," in *Medical Physics*, Vol. 3, 1st ed, edited by O. Glasser (New York, Year Book Publishers, 1944), pp 344–348.
[3]C. Gabriel, S. Gabriel, and E. Corthout, "The dielectric properties of biological tissues. 1. Literature survey," Phys. Med. Biol. **41**(11), 2231–2249 (1996).
[4]S. Gabriel, R. W. Lau, and C. Gabriel, "The dielectric properties of biological tissues. III. Parametric models for the dielectric spectrum of tissues," Phys. Med. Biol. **41**(11), 2271–2293 (1996).
[5]H. P. Schwan, "Electrical properties of tissue and cell suspensions," Adv. Biol. Med. Phys. **V**, 147–209 (1957).
[6]B. Kloesgen, C. Ruemenapp, and B. Gleich, "Bioimpedance spectroscopy," in *BetaSys, System Biology Vol. 2*, edited by B. Booß-Bavnbek *et al.* (Springer-Verlag GmbH, Berlin, 2011), pp. 241–264.
[7]A. J. Portero, "Development of a software application suite for electrical bioimpedance data analysis," Ph.D. thesis, University of Boeras, Sweden, 2010.
[8]J. Jossinett and M. Schmitt, "A review of parameters for the bioelectrical characterization of breast tissue," Ann. N.Y. Acad. Sci. **873**, 30–41 (1999).
[9]N. Chauveau, L. Hamzaoui, P. Rochaix, B. Rigaud, J. J. Voigt, and J. P. Morucci, "*Ex-vivo* discrimination between normal and pathological tissues in human breast surgical biopsies using bioimpedance spectroscopy," Ann. N.Y. Acad. Sci. **873**, 42–50 (1999).
[10]C. Wang, M. Li, and M. Yao, *3rd International Conference on Biomedical Engineering and Informatics (BMEI)* (IEEE, Piscataway, NJ, 2010), pp. 922–926.
[11]K. Wang, X. Dong, F. Fu, Q. Liao, R. Liu, Z. Ji, and T. Wang, "A primary research of the relationship between breast tissues impedance spectroscopy and electrical impedance scanning," *The 2nd International Conference on Bioinformatics and Biomedical Engineering* (IEEE, Piscataway, NJ, 2008), pp. 1575–1579.
[12]J. Estrela da Silva, J. P. Marques de Sá, and J. Jossinet, "Classification of breast tissue by electrical impedance spectroscopy," Med. Biol. Eng. Comput. **38**, 26–30 (2000).
[13]S. Poplack, T. Tosteson, W. Wells, B. Pogue, P. Meaney, A. Hartov, C. Kogel, S. Soho, J. Gibson, and K. Paulsen, "Electromagnetic breast imaging: Results of a pilot study in women with abnormal mammograms," Radiology **243**, 350–359 (2007).
[14]R. Halter, A. Hartov, and K. Paulsen, "A broadband high-frequency electrical impedance tomography system for breast imaging," IEEE Trans. Biomed. Eng. **55**, 650–659 (2008).
[15]R. Halter, T. Zhou, P. Meaney, A. Hartov, R. Barth, Jr., K. Rosenkranz, W. Wells, C. Kogel, A. Borsic, E. Rizzo, and K. Paulsen, "The correlation of *in vivo* and *ex vivo* tissue dielectric properties to validate electromagnetic breast imaging: Initial clinical experience," Physiol. Meas. **30**, S121–S136 (2009).

[16]S. C. Hagness, M. Lazebnik, L. McCartney, D. Popovic, C. B. Watkins, M. J. Lindstrom, J. Harter, S. Sewall, A. Magliocco, J. H. Booske, and M. Okoniewski, "A large-scale study of the ultrawideband microwave dielectric properties of normal, benign and malignant breast tissues obtained from cancer surgeries," Phys. Med. Biol. **52**, 6093–6115 (2007).

[17]M. Lazebnik, L. McCartney, D. Popovic, C. B. Watkins, M. J. Lindstrom, J. Harter, S. Sewall, A. Magliocco, J. H. Booske, M. Okoniewski, and S. C. Hagness, "A large-scale study of the ultrawideband microwave dielectric properties of normal breast tissue obtained from reduction surgeries," Phys. Med. Biol. **52**, 2637–2656 (2007).

[18]O. Casas, R. Bragos, P. Riu, J. Rosell, M. Tresanchez, M. Warren, A. Rodriguez-Sinovas, A. Carreno, and J. Cinca, "*In vivo* and *in situ* ischemic tissue characterization using electrical impedance spectroscopy," Ann. N. Y. Acad. Sci. **873**, 51–58 (1999).

[19]D. Haemmerich, O. Ozkan, J. Tsai, T. Staetlin, S. Tungjitkusolmun, D. Mahvi, and J. Webster, "Changes in electrical resistivity of swine liver after occlusion and postmortem," Med. Biol. Eng. Comput. **40**, 29–33 (2002).

[20]H. P. Schwan, "Electrode polarization impedance and measurements in biological materials," Ann. N. Y. Acad. Sci. **148**(1), 191–209 (1968).

[21]M. Stoneman, M. Kosempa, W. Gregory, C. Gregory, J. Marx, W. Mikkelson, J. Tjoe, and V. Raicu, "Correction of electrode polarization contributions to the dielectric properties of normal and cancerous breast tissues at audio/radiofrequencies," Biol. Med. Phys. **52**, 6589–6604 (2007).

[22]Solartron Analytical, a division of AMETEK, Advanced Measurement Technology unit, B1 Armstrong Mall, Southwood Business Park, Farnborough Hampshire, GU14 0NR, United Kingdom.

[23]Numerical Recipes in C. The art of scientific computing, 2nd Edition, ISBN 0-521-43108-5 (1992).

[24]H. A. Sturges, "The choice of a class interval," J. Am. Stat. Assoc. **21**, 65–66 (1926).

[25]D. Scott, *Multivariate Density Estimation: Theory, Practice, and Visualization* (Wiley, Hoboken, NJ, 1992).

[26]D. Scott, "On optimal and data-based histograms," Biometrika **66**, 605–610 (1979).

[27]D. Freedman and P. Diaconis, "On the histogram as a density estimator: L_2 theory," *Probability Theory and Related Fields* (Springer, Heidelberg, Berlin, 1981), Vol. 57, pp. 453–476.

[28]G. Cumming, F. Fidler, and D. Vaux, "Error bars in experimental biology," J. Cell Biol. **77**(1), 7–11 (2007)

[29]A. Han, L. Yang, and B. Frazier, "Quantification of the heterogeneity in breast cancer cell lines using whole-cell impedance spectroscopy," Clin. Cancer Res. **13**, 139–148 (2007).

[30]G. Qiao, W. Duan, C. Chatwin, A. Sinclair, and W. Wang, "Electrical properties of breast cancer cells from impedance measurements of cell suspensions," J. Phys.: Conf. Ser. **224**(1), 012081 (2010).

[31]H. Subramanian, H. Roy, P. Pradahan, M. Goldberg, J. Muldoon, R. Brand, C. Sturgis, T. Hensing, D. Ray, A. Bogojevic, J. Mohammed, J.-S. Chang, and V. Backman "Nanoscale cellular changes in field carcinogenesis detected by partial wave spectroscopy," Cancer Res. **69**, 5357–5363 (2009).